ARTICLE IN PRESS

Available online at www.sciencedirect.com

ScienceDirect

Surgical Neurology xx (2009) xxx – xxx

SURGICAL NEUROLOGY

www.surgicalneurology-online.com

Aneurysm

Patient-specific hemodynamic analysis of small internal carotid artery-ophthalmic artery aneurysms

Aichi Chien, PhD[a,*], Satoshi Tateshima, MD[a], James Sayre, PhD[b], Marcelo Castro, PhD[c], Juan Cebral, PhD[c], Fernando Viñuela, MD[a]

[a]Division of Interventional Neuroradiology, David Geffen School of Medicine, University of California, Los Angeles, CA 90095, USA
[b]Department of Biostatistics, School of Public Health, University of California, Los Angeles, CA 90095, USA
[c]Department of Computational Sciences, George Mason University, Fairfax, VA 22030, USA

Received 25 July 2008; accepted 31 December 2008

Abstract

Background: Prophylactic treatment of unruptured small brain aneurysms is still controversial due to the low risk of rupture. Distinguishing which small aneurysms are at risk for rupture has become important for treatment. Previous studies have indicated a variety of hemodynamic properties that may influence aneurysm rupture. This study uses hemodynamic principles to evaluate these in the context of ruptured and unruptured small aneurysms in a single location.

Methods: Eight small internal carotid artery-ophthalmic artery (ICA-Oph) aneurysms (<10 mm) were selected from the University of California, Los Angeles, database. We analyzed rupture-related hemodynamic characteristics including flow patterns, wall shear stress (WSS), and flow impingement using previously developed patient-specific computational fluid dynamics software.

Results: Most ruptured aneurysms had complicated flow patterns in the aneurysm domes, but all of the unruptured cases showed a simple vortex. A reduction in flow velocity between the parent artery and the aneurysm sac was found in all the cases. Inside the aneurysms, the highest flow velocities were found either at the apex or neck. We also observed a trend of higher and more inhomogeneous WSS distribution within ruptured aneurysms (10.66 ± 5.99 Pa) in comparison with the unruptured ones (6.31 ± 6.47 Pa) ($P < .01$).

Conclusion: A comparison of hemodynamic properties between ruptured and unruptured small ICA-Oph aneurysms found that some hemodynamic properties vary between small aneurysms although they are similar in size and share the same anatomical location. In particular, WSS may be a useful hemodynamic factor for studying small aneurysm rupture.

Keywords: Cerebral aneurysm; Hemodynamics; Flow analysis; Wall shear stress

1. Introduction

In general, prophylactic treatment of unruptured brain aneurysms remains controversial [9,11,14,25-27]. International studies have shown that the risk of aneurysm rupture increases as the aneurysm size increases, supporting treatment of larger aneurysms [27]. On the other hand, many small aneurysms are observed conservatively due to the lower risk of rupture compared with the risk of morbidity and mortality related to treatments. Recent advancements in medical imaging technology have helped the early detection of unruptured brain aneurysms, and more small aneurysms are found before rupture [2,14]. Among conservatively observed small brain aneurysms, some grow over time with a corresponding increase in the risk of rupture; however, reports have also shown that certain small aneurysms rupture without evidence of any growth [8,13,25]. Although they are

Abbreviations: CFD, computational fluid dynamics; ICA-Oph, internal carotid artery-ophthalmic artery; SD, standard deviation; WSS, wall shear stress.

* Corresponding author. Tel.: +1 310 794 7921; fax: +1 310 206 5958
E-mail address: aichi@ucla.edu (A. Chien).

0090-3019/$ – see front matter © 2009 Published by Elsevier Inc.
doi:10.1016/j.surneu.2008.12.013

similar in diameter, it appears that a subpopulation of small brain aneurysms possess a different rupture risk than others. Identification of small brain aneurysms at high risk for rupture is crucial for evaluating the risks of inaction and treatment [9,15].

Intraaneurysmal hemodynamics has been intensively studied to understand the etiology and natural history of brain aneurysms. In the last decade, a variety of intraaneurysmal hemodynamic research has been published that shows the importance of intraaneurysmal flow characteristics [3,4,6,12,19,20,22,24]. Using patient-specific angiographic data for flow simulation, recent flow analysis studies have suggested that certain hemodynamic parameters, such as flow pattern, flow impingement, and wall shear stress can be used to evaluate the risk of aneurysm rupture [5,19,20,24].

The objective of this research is to use patient-specific hemodynamic simulation to study small aneurysm rupture. Because hemodynamic results are sensitive to aneurysm anatomical location [1,16], to minimize its influence, we compared flow characteristics between ruptured and unruptured small aneurysms at the same anatomical location.

2. Methods

2.1. Case selection

To include as many cases as possible from a single location, we studied the internal carotid artery-ophthalmic artery (ICA-Oph) aneurysm, the most common aneurysm location in our database [17]. A total of 276 patients with ICA-Oph aneurysms who underwent endovascular treatment in the Division of Interventional Neuroradiology, University of California, Los Angeles, Medical Center, from 1996 to 2008 (May) were screened. Patients having angiographic images acquired with sufficient 3-dimensional geometrical detail were selected. A total of 32 in our database satisfied these criteria, and 12 aneurysms met the criteria for small aneurysms, with the greatest diameter less than 10 mm. Because vasospasm may greatly affect the intraaneurysmal hemodynamics, 4 aneurysms with angiographic evidence of vasospasm in the parent artery were excluded [10,21]. Ultimately, 4 ruptured and 4 unruptured small ICA-Oph aneurysms were included in this study.

2.2. Image collection

Aneurysmal 3-dimensional rotational angiography was obtained using a Philips Integris unit (Philips Medical Systems, Best, The Netherlands) before the embolization procedure and then transferred to the Philips Integris workstation for 3-dimensional voxel generation. Because it is difficult to collect images of ruptured aneurysms before the event of rupture, images of ruptured aneurysms were acquired within 24 hours of rupture. Using those images to model ruptured aneurysms, we assumed limited arterial and hemodynamic changes in the 24 hours after rupture.

2.3. Computational fluid dynamics simulation

Image-based computational fluid dynamics (CFD) software developed by researchers at George Mason University (Fairfax, VA) was used for the hemodynamic simulation [5,28]. For each aneurysm, the 3-dimensional voxel data obtained from rotational angiography was first transferred to a Dell 490 workstation, and the computational model was constructed semiautomatically through segmentation, surface generation, and 3-dimensional grid generation. Normal pulsatile flow conditions measured from a healthy subject using magnetic resonance phase contrast measurement were imposed on the model [5]. The unsteady incompressible Navier-Stokes equations were implemented and solved under the Newtonian fluid assumption. Blood was assumed to have uniform viscosity of 0.004 Pa·s. Because information about the aneurysm wall elastic properties is not yet obtainable, the rigid and no-slip boundary condition was assumed for the aneurysm wall in the current simulation [5,19].

Although studies have suggested the importance of incorporating the entire circle of Willis into hemodynamic analysis, this type of simulation has been unable to model small vessels such as ophthalmic arteries [1,5]. To realistically analyze the hemodynamic properties in ICA-Oph aneurysms, models focusing on the internal carotid artery segment incorporating ophthalmic arteries were used. This approach assumed that the flow in the ophthalmic artery has more influence on a ICA-Oph aneurysm than the flow in circle of Willis because this part of the ICA is not within the circle of Willis [1,5].

2.4. Results analysis

The hemodynamic results at the peak of the pulsatile flow time point were carefully examined. The qualitative flow characteristics, such as flow patterns, locations of flow impingement, and impingement size, were evaluated by both AC and ST for each aneurysm. Flow pattern was categorized depending on whether the flow in the aneurysm formed a single vortex or multiple associated vortices. The *flow impingement location* was defined as the position where the inflow jet contacted the aneurysmal wall. It was classified as neck, body, or apex. The impingement size was considered large if the area of impingement was more than half the reference region. For example, if the impingement location was at the neck of the aneurysm, then the impingement size was considered large if the impingement area was larger than half of the neck. Otherwise, the impingement size was recorded as small. Detailed examples of different hemodynamic characteristics can be found in Cebral et al [4].

Values of flow velocity and wall shear stress (WSS) were also compared between ruptured and unruptured cases. To study hemodynamic value changes due to the formation of the aneurysm, hemodynamic results from parent arteries and aneurysm sacs were compared [19]. We obtained hemodynamic results from 6 different locations as indicated

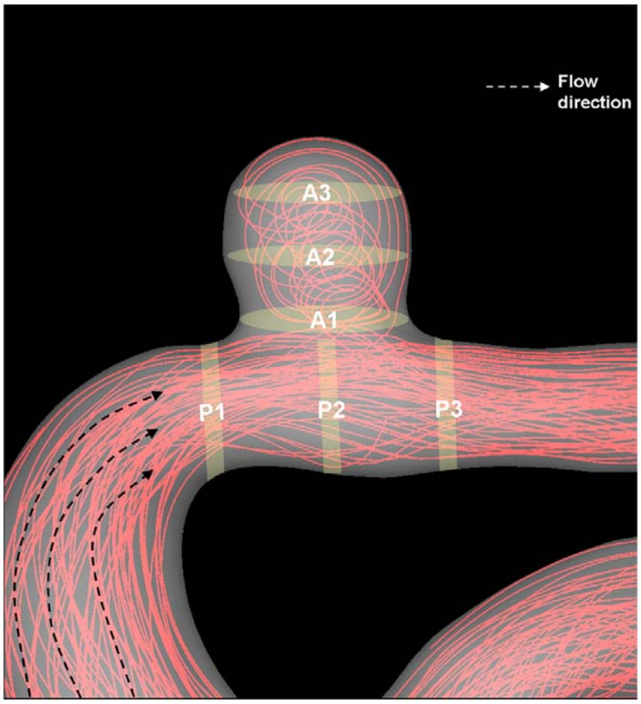

Fig. 1. Schematic representation of aneurysm regions for the quantitative comparisons. Regions in the parent artery were defined evenly spaced at the proximal end of aneurysm sac (P1), center of the aneurysm sac (P2), and distal end of the aneurysm sac (P3). Regions in the aneurysm sac were defined as planes leveled at the neck (A1), middle (A2), and top (A3) of the aneurysm. The distance between these planes is approximately one third of the distance from the neck to the apex of aneurysm.

in Fig. 1. Three different regions in the parent artery were selected—one at the proximal end of the aneurysm dome (P1), the center of the aneurysm dome (P2), and at the distal end of the aneurysm dome (P3). Likewise, 3 regions in the aneurysm were selected at the neck of aneurysm (A1), at the middle region of the aneurysm (A2), and at the top of the aneurysms (A3).

2.5. Statistical analysis

Quantitative results are expressed as mean value and SD. Multivariate tests were performed for comparisons with the ruptured and unruptured aneurysm data using the SPSS 13.0 statistical software (SPSS Inc, Chicago, IL). Statistical significance was indicated at the 1% level.

3. Results

3.1. Blood flow characteristics

Flow patterns at the peak of pulsatile flow are shown in Fig. 2. Cases 1 to 4 and cases 5 to 8 are ruptured and unruptured aneurysms, respectively. All of the unruptured aneurysms had blood inflow into the aneurysm forming a single vortex. In the ruptured cases, only one had a single vortex (case 2); the other aneurysms had blood inflow with multiple associated vortices (Table 1). Five aneurysms had blood flow impinging at the neck (3 ruptured and 2 unruptured), 2 at the body (1 ruptured and 1 unruptured), and 1 at the apex of the aneurysm (unruptured). Overall, half

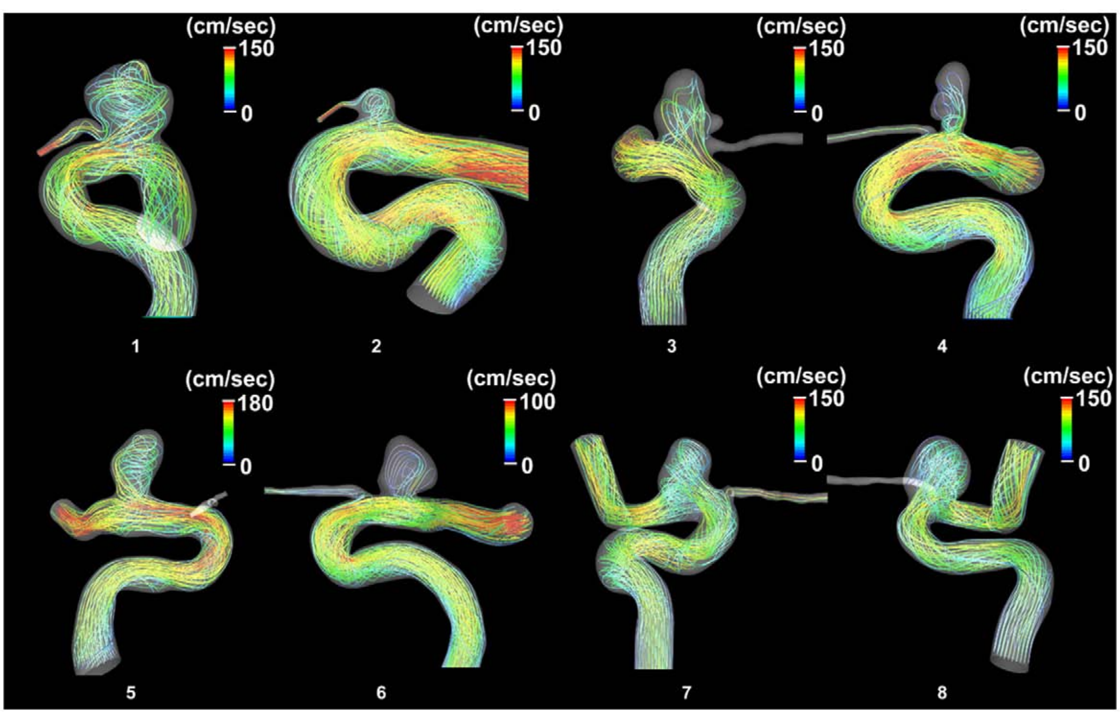

Fig. 2. Blood flow patterns in ruptured aneurysms (top, case 1-4) and unruptured aneurysms (bottom, case 5-8). Among the aneurysms, cases 1, 3, and 4 showed a blood flow pattern with multiple vortices. The rest of the aneurysms had a single vortex. Cases 1, 2, and 4 to 6 had blood flow impingement at the neck of the aneurysm. Cases 3 and 7 had blood flow impingement at the body of the aneurysm. Case 8 had blood flow impingement at the dome of the aneurysm.

Table 1
Blood flow characteristics in ruptured and unruptured aneurysms

	Ruptured	Unruptured	Total
n	4	4	8
Flow direction			
Single vortex	1	4	5
Multiple vortices	3	0	3
Impingement location			
Neck	3	2	5
Body	1	1	2
Apex	0	1	1
Impingement size			
Small	2	2	4
Large	2	2	4
WSS pattern in aneurysm region			
High at aneurysm dome	4	0	4
Low at aneurysm dome	0	4	4

of the aneurysms showed a small blood flow impingement size. We did not find a distinguishable difference in impingement location and size between the ruptured and unruptured cases.

3.2. Wall shear stress distribution

Fig. 3 shows the WSS distribution of aneurysms. We found that in the ruptured aneurysms (cases 1-4), the WSS was higher and distributed more inhomogeneously in the aneurysm sacs. Around the neck of most ruptured aneurysms, there was an area of WSS with magnitude similar to the parent artery, which then broadened from the neck to the body of the aneurysm. In contrast, in the unruptured aneurysms (cases 5-8), the WSS throughout the aneurysm sacs was much lower than the WSS at the parent arteries. Unruptured aneurysms also usually had a border of low WSS (dark blue) around the neck. Local, low WSS was observed at some bulb regions (cases 3 and 4), but some high WSS bulbs were also seen (cases 1 and 4).

3.3. Quantitative comparison

Fig. 4 shows the flow velocity at different areas of each aneurysm. Fig. 4A shows the flow velocity in the parent artery, and Fig. 4B shows the flow velocity in the aneurysm sacs. In general, the blood flow velocity was high before entering the aneurysm (P1). Then, flow velocity in the parent artery decreased at the aneurysm region (P2). Distal to the aneurysm, the high flow velocity in the parent arteries returned (P3). In Fig. 4A and B, a reduction in flow velocity between the parent artery and the aneurysm sac is visible in all cases. The highest flow velocity inside an aneurysm was either at the apex (A3) or the neck (A1) of the aneurysms. Notably, the aneurysms with the highest velocity at the aneurysm apex (A3) were ruptured aneurysms (cases 1-3). The average flow velocities in ruptured aneurysms were 63.20 ± 29.89 cm/s in parent arteries and 38.56 ± 18.38 cm/s in aneurysm sacs. The average flow velocities in unruptured aneurysms were 51.98 ± 18.64 cm/s in parent arteries and 35.46 ± 24.59 cm/s in aneurysm sacs. On this scale, there was no significant difference in flow velocity between ruptured and unruptured aneurysms.

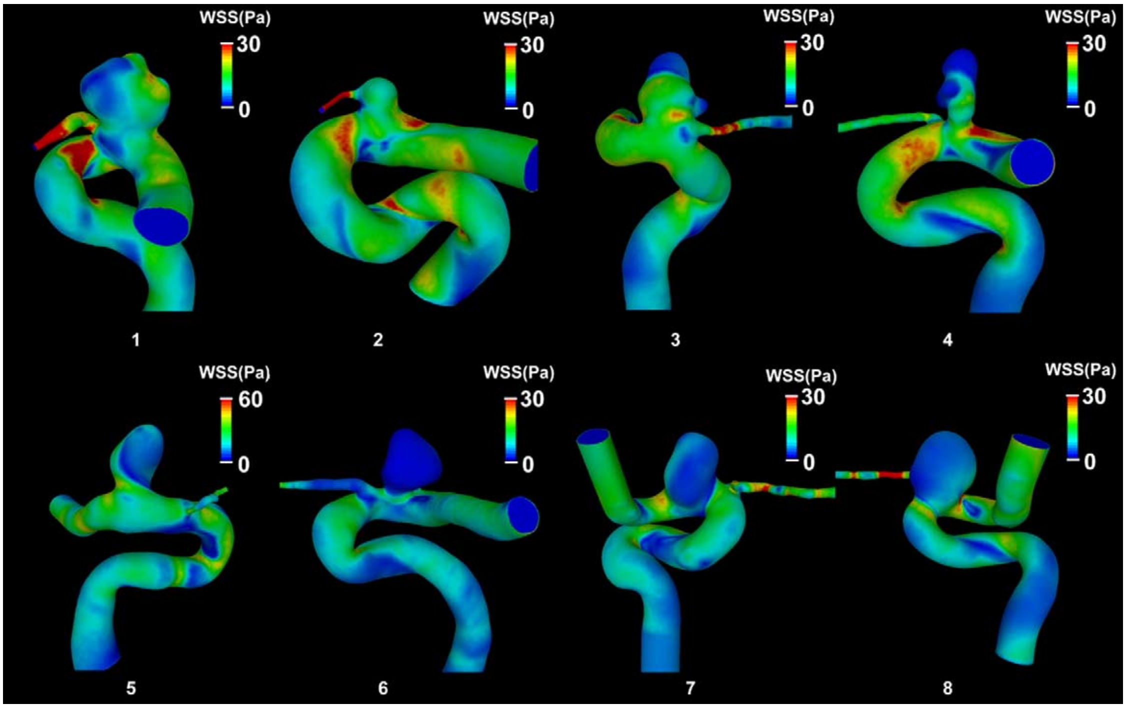

Fig. 3. Wall shear stress distributions in ruptured aneurysms (top, case 1-4) and unruptured aneurysms (bottom, case 5-8). Inhomogeneous and higher WSS were found in the ruptured aneurysms. In unruptured aneurysms, large areas of low WSS (dark blue) were found at the aneurysm sacs.

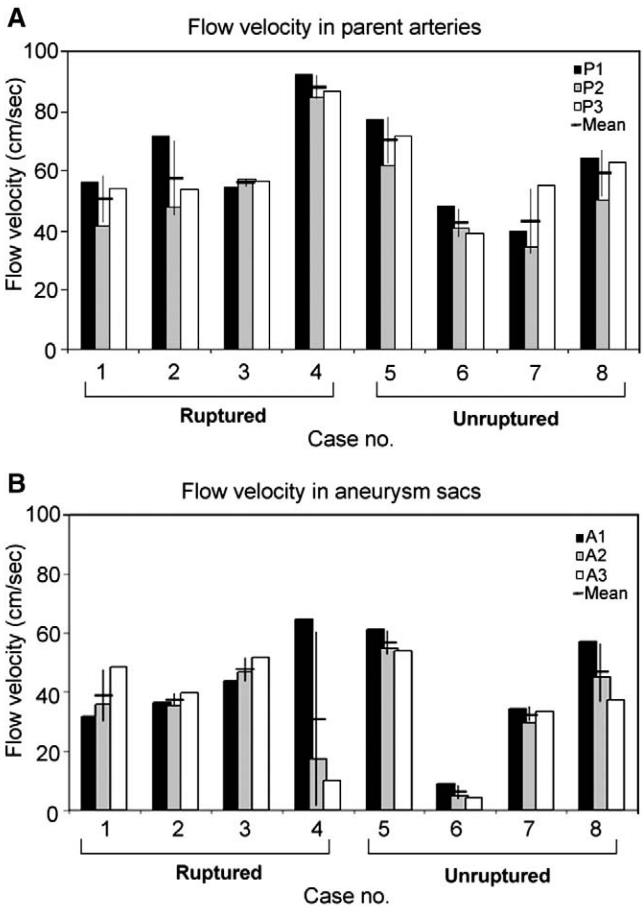

Fig. 4. Flow velocity in different regions of the aneurysms. Numbers correspond to the cases shown in Fig. 2. Cases 1 to 4 are ruptured aneurysms. Cases 5 to 8 are unruptured aneurysms. P1, P2, P3, A1, A2, and A3 are shown in Fig. 1. A: Flow velocity in the parent arteries. B: Flow velocity in aneurysm sacs. Reduction of flow velocity from the parent artery to the aneurysm sacs was found in every aneurysm, but there was no clear difference between ruptured and unruptured cases.

Fig. 5 shows the WSS at different regions of parent artery (5A) and aneurysm sac (5B). It shows that the highest WSS area near an aneurysm is usually the proximal region in the parent artery (P1). Within an aneurysm, the highest WSS often occurs at the neck (A1). The reduction of WSS from the parent artery to the aneurysm sac can be observed in Fig. 5A and B. The average WSS in ruptured aneurysms was 14.11 ± 6.56 Pa in parent arteries and 10.66 ± 5.99 Pa in aneurysm sacs. The average WSS in unruptured aneurysms was 14.07 ± 7.05 Pa in parent arteries and 6.31 ± 6.47 Pa in aneurysm sacs. Comparison of WSS in ruptured and unruptured aneurysms showed that the WSS in the aneurysm sac was much higher in ruptured aneurysms (Fig. 5B, case 1-4) than unruptured aneurysms (Fig. 5B, case 5-8) ($P < .01$).

4. Discussion

Development of aneurysms is associated with the vascular wall response to various hemodynamic stresses [18,19,23]. Using experimental measurement or computer simulation, hemodynamic parameters such as the flow velocity and WSS can be obtained based on fluid dynamics principles. These hemodynamic parameters may help determine not only the mechanical effect of blood flow on the vessels but also how the molecular response within the vessel wall is associated with the physical forces caused by the blood flow.

In this study, we examined flow properties reported to relate to aneurysm rupture and compared them within ruptured and unruptured small aneurysms. As previous research found, more complicated flow patterns were observed in the ruptured aneurysms [4]. We also observed that ruptured small aneurysms tended to have multiple vortices circulating in the aneurysm domes. However, no clear difference in impingement properties between ruptured and unruptured small aneurysms was found. Further studies restricted to small aneurysms with more cases may clarify this observation. Because impingement properties were initially identified as a factor related to aneurysm rupture in analyses of aneurysms from various locations and sizes, it

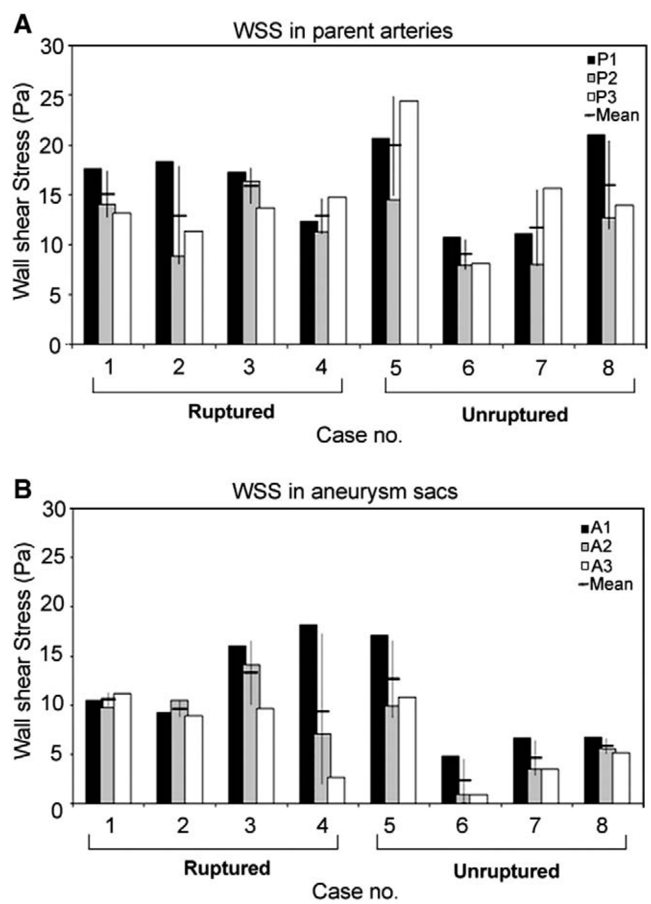

Fig. 5. Wall shear stress in different regions of the aneurysms (the same arrangement as Fig. 4). A: WSS in the parent arteries. B: WSS at the aneurysm sac. Reduction of the WSS from parent artery to the aneurysm sac was observed. Higher WSS in the ruptured aneurysm sacs (case 1-4) was found.

is possible that they may not be particularly strong indicators of the risk of small aneurysm rupture [4].

Blood flow in the vascular system causes a frictional force acting on the vessel wall, WSS, which elicits strong physiologic responses on a molecular scale [7,18]. In this study, we analyzed the blood flow before and after entering the aneurysm sac, and the WSS around the aneurysm area, to characterize the flow changes around the aneurysms and the corresponding frictional force. We found the same flow velocity changes around the aneurysm in all cases and no clear difference between ruptured and unruptured aneurysms. On the other hand, although for all the cases, the WSS in the aneurysm sac was lower than the WSS in the parent artery on average, the difference was less pronounced in ruptured aneurysms. Ruptured aneurysms had WSS of 75.33% lower than the parent artery, whereas unruptured aneurysms had WSS of 41.19% lower than the parent artery. Further studies incorporating molecular response in the aneurysm wall may help to explain the influence of different WSS levels. Still, the present study suggests that among rupture-related hemodynamic properties, WSS may be a useful hemodynamic parameter to evaluate the risk of rupture in small brain aneurysms.

4.1. Limitations

We performed hemodynamic analysis on 8 aneurysm cases in a single location. Because of the limited number of cases, the present study can only show the trend of hemodynamic properties in small aneurysms. A study with more cases, for example, combining databases from different centers, is needed to confirm our observation. Moreover, because aneurysms in other locations may have different flow characteristics, analyses for small aneurysms in other locations may also be needed.

5. Conclusion

Hemodynamic analyses of small aneurysms enabled us to compare the detailed blood flow characteristics between ruptured and unruptured cases. We found that not all aneurysms that are small share the same hemodynamic properties. Among the characteristics investigated, the value of WSS in an aneurysm sac was the only hemodynamic parameter that showed statistical differences between ruptured and unruptured aneurysms.

References

[1] Alnaes MS, Isaksen J, Mardal KA, et al. Computation of hemodynamics in the circle of Willis. Stroke 2007;38:2500-5.

[2] Brisman JL, Song JK, Newell DW. Cerebral aneurysms. N Engl J Med 2006;355:928-39.

[3] Burleson AC, Strother CM, Turitto VT. Computer modeling of intracranial saccular and lateral aneurysms for the study of their hemodynamics. Neurosurgery 1995;37:774-82 [discussion 782-4].

[4] Cebral JR, Castro MA, Burgess JE, et al. Characterization of cerebral aneurysms for assessing risk of rupture by using patient-specific computational hemodynamics models. AJNR Am J Neuroradiol 2005; 26:2550-9.

[5] Cebral JR, Castro MA, Soto O, et al. Blood-flow models of the circle of Willis from magnetic resonance data. J Eng Math 2003;47:369-86.

[6] Cebral JR, Lohner R. Efficient simulation of blood flow past complex endovascular devices using an adaptive embedding technique. IEEE Trans Med Imaging 2005;24:468-76.

[7] Cheng C, Tempel D, van Haperen R, et al. Atherosclerotic lesion size and vulnerability are determined by patterns of fluid shear stress. Circulation 2006;113:2744-53.

[8] Dhaliwal S, Sylvester L, Pope W, et al. The natural history of unruptured cerebral aneurysms studied longitudinally using helical CT angiography. Chicago (Ill): Radiological Society of North America; 2003. p. 284.

[9] Donnan GA, Davis SM. Patients with small, asymptomatic, unruptured intracranial aneurysms and no history of subarachnoid hemorrhage should be treated conservatively. Stroke 2005;36:407.

[10] Humphrey JD. Vascular adaptation and mechanical homeostasis at tissue, cellular, and sub-cellular levels. Cell Biochem Biophys 2008; 50:53-78.

[11] Johnston SC, Gress DR, Kahn JG. Which unruptured cerebral aneurysms should be treated? A cost-utility analysis. Neurology 1999;52:1806-15.

[12] Jou LD, Quick CM, Young WL, et al. Computational approach to quantifying hemodynamic forces in giant cerebral aneurysms. AJNR Am J Neuroradiol 2003;24:1804-10.

[13] Juvela S, Porras M, Heiskanen O. Natural history of unruptured intracranial aneurysms: a long-term follow-up study. J Neurosurg 1993;79:174-82.

[14] Juvela S, Porras M, Poussa K. Natural history of unruptured intracranial aneurysms: probability of and risk factors for aneurysm rupture. J Neurosurg 2000;93:379-87.

[15] Kataoka K, Taneda M, Asai T, et al. Difference in nature of ruptured and unruptured cerebral aneurysms. Lancet 2000;355:203.

[16] Kayembe KN, Sasahara MHazama F. Cerebral aneurysms and variations in the circle of Willis. Stroke 1984;15:846-50.

[17] Murayama Y, Nien YL, Duckwiler G, et al. Guglielmi detachable coil embolization of cerebral aneurysms: 11 years' experience. J Neurosurg 2003;98:959-66.

[18] Papaioannou TG, Karatzis EN, Vavuranakis M, et al. Assessment of vascular wall shear stress and implications for atherosclerotic disease. Int J Cardiol 2006;113:12-8.

[19] Shojima M, Oshima M, Takagi K, et al. Magnitude and role of wall shear stress on cerebral aneurysm: computational fluid dynamic study of 20 middle cerebral artery aneurysms. Stroke 2004;35:2500-5.

[20] Shojima M, Oshima M, Takagi K, et al. Role of the bloodstream impacting force and the local pressure elevation in the rupture of cerebral aneurysms. Stroke 2005;36:1933-8.

[21] Soustiel JF, Levy E, Bibi R, et al. Hemodynamic consequences of cerebral vasospasm on perforating arteries: a phantom model study. Stroke 2001;32:629-35.

[22] Steinman DA, Milner JS, Norley CJ, et al. Image-based computational simulation of flow dynamics in a giant intracranial aneurysm. AJNR Am J Neuroradiol 2003;24:559-66.

[23] Tateshima S, Murayama Y, Villablanca JP, et al. In vitro measurement of fluid-induced wall shear stress in unruptured cerebral aneurysms harboring blebs. Stroke 2003;34:187-92.

[24] Tateshima S, Murayama Y, Villablanca JP, et al. Intraaneurysmal flow dynamics study featuring an acrylic aneurysm model manufactured using a computerized tomography angiogram as a mold. J Neurosurg 2001;95:1020-7.

[25] Tsutsumi K, Ueki K, Morita A, et al. Risk of rupture from incidental cerebral aneurysms. J Neurosurg 2000;93:550-3.

[26] Wermer MJ, van der Schaaf IC, Algra A, et al. Risk of rupture of unruptured intracranial aneurysms in relation to patient and aneurysm characteristics: an updated meta-analysis. Stroke 2007; 38:1404-10.

[27] Wiebers DO, Whisnant JP, Huston III J, et al. Unruptured intracranial aneurysms: natural history, clinical outcome, and risks of surgical and endovascular treatment. Lancet 2003;362:103-10.

[28] Yim P, Demarco K, Castro MA, et al. Characterization of shear stress on the wall of the carotid artery using magnetic resonance imaging and computational fluid dynamics. Stud Health Technol Inform 2005;113: 412-42.

Commentary

The authors have presented a very interesting and potentially clinically valuable technique for the study of intracranial aneurysms. Using their methods, they found statistically significant differences in wall shear stress between ruptured and unruptured ophthalmic aneurysms and identified other differences that did not quite reach statistical significance. The technique, which involves modeling of hemodynamic parameters from high-resolution angiograms, is potentially clinically important because we currently do not have methods for segregating small aneurysms into groups with higher or lower rupture probability.

We believe that aneurysm diameter is the most important determinant of rupture probability and that the potential for rupture increases as the third power of diameter. However, although most small aneurysms do not rupture, a small fraction of them do. Perhaps analysis of wall shear stress or other hemodynamic parameters will help determine which aneurysms of a given small diameter are more likely to rupture and deserve prophylactic treatment.

Obviously, the authors need to improve their techniques so that they can study larger groups of aneurysms. Furthermore, it would be valuable if their databases included some cases that were studied both before and after rupture because with the current data it is difficult to exclude the possibility that differences in wall shear stress were a result of rupture rather than causative. However, the techniques and approach presented in this article deserve careful consideration and have the potential to significantly add to our ability to decide which small lesions should be treated.

Phillip Dickey, MD
Kailasnath Purushothaman, PhD
Yale School of Medicine
New Haven, CT 06510, USA

This article compared the hemodynamic properties for ruptured and unruptured aneurysms by simulating the hemodynamics of small (<10 mm) internal carotid artery-ophthalmic artery aneurysms using an image-based computer fluid dynamics software. They found a higher and more inhomogeneous wall shear stress distribution in the ruptured aneurysms when compared to the unruptured ones. This gives us more information about how to predict which aneurysms will rupture—at least evidence based more than just the size of the aneurysm.

As with all mathematical models, assumptions are made so as to represent as accurately as possible the biologic system properties. The authors have addressed some of these concerns in their Methods section. The article also uses a small sample size, which subjects its conclusions to some limitations. In general, however, this article lays the groundwork for further studies for looking at how hemodynamic parameters can be used to predict which aneurysms are at higher risks for rupture.

Kern H. Guppy, MD, PhD
Division of Neurosurgery
Kaiser Permanente/UCSF
Sacramento, CA 95825, USA